

CO emission from discs around isolated HAeBe and Vega-excess stars

W. R. F. Dent¹, J. S. Greaves¹, I. M. Coulson²

¹*UK Astronomy Technology Centre, Royal Observatory, Blackford Hill, Edinburgh EH9 3HJ, Scotland*

²*Joint Astronomy Centre, 660 N. A'ohoku Place, Hilo, Hawaii 96720, USA*

30 September 2018

ABSTRACT

We describe results from a survey for J=3-2 ¹²CO emission from visible stars classified as having an infrared excess. The line is clearly detected in 21 objects, and significant molecular gas ($\geq 10^{-3}$ Jupiter masses) is found to be common in targets with infrared excesses ≥ 0.01 (≥ 56 per cent of objects), but rare for those with smaller excesses (~ 10 per cent of objects).

A simple geometrical argument based on the infrared excess implies that disc opening angles are typically $\geq 12^\circ$ for objects with detected CO; within this angle, the disc is optically thick to stellar radiation and shields the CO from photodissociation. Two or three CO discs have an unusually low infrared excess (≤ 0.01), implying the shielding disc is physically very thin ($\leq 1^\circ$).

Around 50 per cent of the detected line profiles are double-peaked, while many of the rest have significantly broadened lines, attributed to discs in Keplerian rotation. Simple model fits to the line profiles indicate outer radii in the range 30-300 au, larger than found through fitting continuum SEDs, but similar to the sizes of debris discs around main sequence stars. As many as 5 have outer radii smaller than the Solar System (50 au), with a further 4 showing evidence of gas in the disc at radii smaller than 20 au. The outer disc radius is independent of the stellar spectral type (from K through to B9), but there is evidence of a correlation between radius and total dust mass. Also the mean disc size appears to decrease with time: discs around stars of age 3-7 Myr have a mean radius ~ 210 au, whereas discs of age 7-20 Myr are a factor of 3 smaller. This shows that a significant mass of gas (at least $2M_\oplus$) exists beyond the region of planet formation for up to ~ 7 Myr, and may remain for a further ~ 10 Myr within this region.

The only bona fide debris disc with detected CO is HD9672; this shows a double peaked CO profile and is the most compact gas disc observed, with a modelled outer radius of 17 au. In the case of HD141569, detailed modelling of the line profile indicates gas may lie in two rings, with radii of 90 and 250 au, similar to the dust structure seen in scattered light and the mid-infrared. In both AB Aur and HD163296 we also find the sizes of the molecular disc and dust scattering disc are similar; this suggests that the molecular gas and small dust grains are closely co-located.

Key words: stars: lines - spectra.

1 INTRODUCTION

Vega-excess stars were initially identified as being apparently normal main-sequence stars with an excess of emission above that of the photosphere at $\lambda \geq 12 \mu\text{m}$ (Aumann et al., 1984). Several lists of these objects have been compiled, such as that of Mannings & Barlow (1998), who cross-compared the IRAS Faint Source and the Michigan Spectral Cata-

logues. They found a total of ~ 110 stars with detectable excesses, of which around 60 per cent are of spectral type B or A. Their Spectral Energy Distributions (SEDs) are very similar to many objects at the later stages of pre-main-sequence evolution, such as Herbig AeBe stars. HAeBe stars have spectral types later than B8 with clear optical emission lines and nearby nebulosity, both indicative of youth (Herbig, 1960). They are assumed to be the high-mass equiva-

lents of T Tauri stars. Thé et al. (1994) identified ~ 115 bona fide HAeBe candidates, and extended the spectral range to Fe stars. Many of the classical HAeBe stars are associated with nearby star formation, such as ambient molecular gas, optical nebulosity, outflows or infalling envelopes; typically this is found at radii of $\sim 10^3 - 10^6$ au, and so can confuse studies of the stars themselves. However, Grinen et al. (1991), Meeus et al. (2001) and others identified a subclass of these stars which are relatively isolated, having no nearby cloud and a low line-of-sight extinction. The absence of nearby active star formation suggests that they are older than their classical brethren. Comparison with stellar evolutionary tracks give ages of a few Myr (e.g. van den Ancker et al., 1998), as compared with $10^4 - 10^5$ yr for classical HAeBe stars (eg Fuente et al., 2002; Greaves et al., in prep.). Observations of these isolated stars are easier to interpret as their circumstellar disc emission is less confused by the ambient gas envelope (e.g. Dominik et al., 2003).

Because of the similarity of the SEDs, there is some confusion in the classification of Vega-excess and HAeBe stars. Dunkin et al. (1997) and Coulson et al. (1998) suggested some of the “dusty” Vega-excess objects are actually at an intermediate stage between HAeBe and main-sequence Vega-type stars. This class of isolated HAeBe star or dusty Vega-excess object may be therefore lie at an important evolutionary stage at the end of the pre-main-sequence phase, and are therefore sometimes known as “transition” objects (e.g. Malfait et al., 1998).

The material around HAeBe and Vega-excess stars is most commonly studied in dust continuum emission. However, molecular gas - traced by the low-J lines of CO - has also been detected in a small number of objects (e.g. Zuckerman et al., 1995; Coulson et al., 1998; Greaves et al., 2000; Thi et al., 2001). In many cases the signal:noise has been too low to obtain details of the line profiles, although some show a double-peaked line. In five of the brightest objects, the line emission has been resolved using mm-wave interferometry, revealing that the gas is located in a rotating disc (Manning & Sargent, 1997, 2000; Piétu et al., 2003). A disc would also explain the simultaneous high fractional excess emission, and low visual extinction (e.g. van den Ancker et al., 1998). Attempts to detect mm-wave CO emission from the archetypal Vega-excess stars such as Vega and β Pictoris have proved unsuccessful, with measured CO/dust depletions of more than 10^3 (Dent et al., 1995; Liseau, 1999). This is likely to be caused by photodissociation from stellar UV; however if there remain some regions of the disc where the optical extinction to the star and interstellar radiation field is ≥ 3 mag, significant CO could still be present (e.g. Greaves et al., 2000; Kamp et al., 2003).

The following observations comprise a more general survey of infrared excess stars for molecular gas, as traced by the J=3-2 transition of ^{12}CO . Targets are identified as either Vega-excess or isolated HAeBe stars. We have then compared the line profiles with a simple disc model to determine some of the basic system parameters.

2 OBSERVATIONS

The data were taken using the facility heterodyne receiver RxB3 on the JCMT. Observations were made at the ^{12}CO

J=3-2 line rest frequency of 345.796 GHz, using the secondary chopper to obtain a sky reference 150 arcsec distant in azimuth. Spectra from both orthogonally-polarised mixers were averaged together. Total integration times were 30 or 60 minutes, although a few selected stars were targeted for longer integrations (up to 8 hours) to better delineate the line shapes. Most data were obtained as part of a poor-weather backup program carried out between 2000 September and 2001 January, and 2003 January to April. A few longer integration observations of selected targets were carried out in 2004 June. Additional data were also obtained from the JCMT archive, a subset of which has previously been published (Coulson et al., 1998; Greaves et al., 2000; Thi et al., 2001). In these cases, we have coadded the existing JCMT data with the new results in order to increase the effective integration time.

The target list was taken from the following surveys:

- The list of Vega-like systems with bright IRAS excesses from Sylvester et al. (1996) (17 out of their 24 stars).
- Young (1-10 Myr) stars with associated dust from Zuckerman et al. (1995) (13 out of 16 stars).
- Vega-excess stars with the largest far-infrared flux from Mannings & Barlow (1998).
- Isolated HAeBe stars from Malfait et al. (1998), van den Ancker et al. (1998) and Grady et al. (1996).

As mentioned above, in many cases the simple identification of a star as luminosity Class V with an IRAS excess means that the target list includes both isolated Herbig HAeBe or even T Tauri stars, as well as Vega-excess stars. We have avoided the classical embedded HAeBe stars. In addition, a small number of stars have subsequently been identified being luminosity Class III or IV, or have revised distance estimates; these have been identified in the analysis.

The basic target information and results are given in Table 1; distances in most cases are from the Hipparcos catalogue and when not available we have used literature values or those derived from the visual magnitude. Also listed are the fractional excess luminosities, f , ie the luminosity radiated from the system in excess of the photosphere, as a fraction of the total stellar photospheric emission. In most cases f is obtained from the literature, or by fitting modified black-bodies to the available optical through to sub-mm fluxes. This fitting assumes in most cases a single temperature for the dust, with an opacity index, $\beta = 1.0$ (e.g. Dent et al., 2000). The typical uncertainty in the fractional excess is estimated to be a factor of two, mostly due to the incomplete wavelength coverage.

The CO integrated emission or $1-\sigma$ upper limits are given in the Table. In the case of a line detection, the centroid CO velocity and the stellar velocity from the literature are also listed. In most cases these are in reasonable agreement, giving confidence that the observed gas is associated with the star and not with background Galactic emission. Despite the targetting of isolated objects, 3 or 4 objects showed bright, narrow positive or negative lines, indicating an extended ambient cloud either associated with the star or along the line of sight.

Table 1. Target stars and observational results.

HD	Other name	Sp. type ⁽¹⁾	d ⁽²⁾ (pc)	f ⁽³⁾	CO intensity ⁽⁴⁾ (K km s ⁻¹)	v _{CO} (km s ⁻¹)	v _* (km s ⁻¹)	Notes ⁽⁷⁾ & references
627		B7V	403v	1.1×10 ⁻³	<0.16			Nearby star formation. J01
4881		B9.5V	168r	1.9×10 ⁻³	0.12±0.05	-15.3	-13.7±2	S(0.98). Poss. cirrus. K02
6028		A3V	91v	1.1×10 ⁻³	<0.15			
9672	49 Cet	A1V	61	8.7×10 ⁻⁴	0.34±0.07	10.5	9.9	D. Z95,S96,MS00
17081		B7IV	135	1.3×10 ⁻⁴	<0.064			
23362		K5III	308	7.9×10 ⁻⁴	<0.19			Poss. cirrus. S96,K02
23680		G5IV	180	3.0×10 ⁻³	<0.15			S96
31293	AB Aur	A0V	144	0.48	7.4±0.17	15.1	8±5	D. MS97,M01
31648	MWC480	A5V	131	0.2	2.74±0.06	14.5	-	D. MS97,S01
32509		A2V	150	0.016	<0.11			
34282		A0.5V	400r	0.39	1.1±0.12	16.2	-	D. PDK03,S96
34700		G0IV	125r	0.15	0.42±0.06	21.0	-	D. S96,CWD98,SDB01,T04
35187		A2V	150	0.16	<0.26			Binary. J01,DC98.
35929		F0III	400r	0.011	<0.048			vdA98
36112	MWC758	A3V	204	0.17	0.81±0.1	17.0	17.6±0.2	S(2.4). MS97,T01,B99
36910	CQ Tau	F5IV	99	0.25	0.31±0.05	17.7	20	D? N01,MS00
37806		B9V	280v	0.32	<0.14			M98
38120		B9V	420r	0.47	0.66±0.12	31.6	-	S(1.4). CWD98
48682		G0V	16	1.2×10 ⁻⁴	<0.11			
50138		B8V ⁽⁶⁾	289	0.6	<0.074			Poss. Be star
53833		A9V	267v	0.02	<0.25			IR not near star. SM00
58647		B9IV	280	0.15	<0.11			Poss. Be star
81515		A5V	106	6.1×10 ⁻³	<0.09			
98800		K4V	46	0.084	<0.09			S96
102647	β Leo	A3V	11	1.9 × 10 ⁻⁵	<0.18			J=2-1 CO. J01, D95
109085		F2V	18	6.9×10 ⁻⁵	<0.08			
121847	47 Hya	B8V	104	2.4 × 10 ⁻⁴	<0.07			
123247		B9.5V	101	1.3×10 ⁻⁴	<0.3			
123356		G1V	41	6.1×10 ⁻³	<0.07			
135344	SAO206462	F4V	84r	0.44	0.97±0.04	2.9	-3±3	D. S96,CWD98,T01,M01,D03
139365		B2.5V	136	1.4×10 ⁻⁵	<0.063			
139450		G0/1V	73	2.4×10 ⁻³	-			Ambient emission
139614		A7V	157r	0.39	0.47±0.11	3.3	3±1	S? S96,M01,D03
141569		A0V	99	8.4×10 ⁻³	0.76±0.055	-7.5	-6±5	D. S96, L03
142114		B2.5V	132	7.5×10 ⁻⁵	<0.07			
142165		B5V	127	4.0×10 ⁻⁵	<0.064			
142666		A8V	116r	0.28	0.72±0.14	-5.0	3±1	S?(4.9). S96,M01,D03
143006		G5V	82r	0.37	0.15±0.06	-0.8	-0.9±0.3	S(0.95). J01,S96
143018		B1V	140	1.5×10 ⁻³	<0.14			
144432		A9V	200	0.26	0.31±0.13	-2.2	2±3	D? S96,M01,D03
145718	V718 Sco	A8IV ⁽⁶⁾	130	0.1	0.45±0.23	-4.2	-	D? Marginal det. Z95,T01
150193	MWC863	A1V	150	0.15	<0.07			Poss. ambient emission. M01
155826		G0V	30	6.5×10 ⁻⁴	-			Bright ambient em. L02
163296		A1V	122	0.16	4.3±0.1	-6.4	-4±1	D. MS97,M01,J01
169142		A5V	145r	0.1	1.7±0.13	-3.1	-3±2	S(1.6). M01,D03
179218	MWC614	A0IV	243	0.62	0.6±0.12	16.1	-3±5	D. M01
190073	MWC325	A2IV	400	0.4 ⁽⁵⁾	<0.08			
191089		F5V	53	2.3×10 ⁻³	<0.25			
212676		B9V	670	4.7×10 ⁻³	<0.08			CWD98
214953		G0V	23	2.3×10 ⁻⁴	<0.28			
215592		A0V ⁽⁶⁾	590r	0.048	0.18±0.12	1.7	2.7±5	Marginal detection. CWD98
224648		B9V ⁽⁶⁾	300	8.7 × 10 ⁻³	<0.085			
232344		B9V ⁽⁶⁾	450	0.086	<0.09			
233517		K5III	600r	0.057	0.21±0.11	36.0	46.5±1	S(3.6). S01,F96
287841	V346 Ori	A2IV	400	0.1	<0.06			
293782	UX Ori	A4IV	430	0.35	0.21±0.07	17.2	18.3	S(0.98). CO at v=27. N01
344361	WW Vul	A2IV	370	0.42	<0.095			N01
-	VX Cas	A0V	760	0.3 ⁽⁵⁾	<0.09			
-	TW Hya	K7e	56	0.3	2.16±0.2	12.35	12.6	S. K97

Notes to Table 1:

- (1) Spectral types are either from Moro et al. (2001), from the references given, or from the Simbad database.
- (2) Distances are normally from Hipparcos, except those marked ‘r’, which are taken from the given reference, or ‘v’ estimated from visual magnitude, uncorrected for reddening.
- (3) Fraction excess is taken from the literature, or where not available, estimated from a fit to the SED (see text for details).
- (4) Intensity units are main beam brightness temperature (using $\eta_{\text{mb}} = 0.62$). To calculate the upper limits, the rms noise has been measured with 10 km s⁻¹ channels; 1- σ values are given.
- (5) Estimate of fractional excess is uncertain, due to wide range of temperatures in excess emission, possibly high extinction to star and/or incomplete wavelength coverage.
- (6) Luminosity classification based on distance and optical magnitude.
- (7) For targets with detected CO, an indication is given of whether the line is double-peaked (D) or single-peaked (S). In the case of single lines, the linewidth (FWHM) is also given (in km s⁻¹).

References:

B99: Beskrovnaya et al., (1999); CWD98: Coulson et al. (1998); D03: Dominik et al. (2003); DC98: Dunkin & Crawford (1998); F96: Fekel et al. (1996); G00: Greaves et al. (2000); J01: Jayawardhana et al. (2001); K02: Kalas et al. (2002); K97: Kastner et al. (1997); L02: Lisse et al., (2002); L03: Li & Lunine (2003); M98: Malfait et al., (1998); M01: Meeus et al. (2001); MS97: Mannings & Sargent (1997); MS00: Mannings & Sargent (2000); N01: Natta et al. (2001); PDK03: Piétu, Dutrey, Kahane (2003); S01: Simon et al. (2001); SDB01: Sylvester, Dunkin & Barlow (2001); S96: Sylvester et al. (1996); SM00: Sylvester & Mannings (2000); T01: Thi et al. (2001); T04: Torres (2004); vdA98: van den Ancker et al. (1998); Z95: Zuckerman et al. (1995).

3 DETECTABILITY OF CO

A total of 59 targets were observed, of which 21 were detected in CO with 2 additional marginal detections (at the 2- σ level). In Fig. 1, we plot I_{CO} , the measured CO intensity or 1- σ limit normalised to a distance of 100 pc, as a function of the fractional infrared excess f . The normalisation of the CO line intensity assumes the emission to be smaller than the beam; the emitting regions are typically a few hundred au in radius (see below), which compares with the beam size of 1400 au at a distance of 100 pc. As the ¹²CO line is likely to be optically thick (see below), the normalised CO intensity can be used to estimate a lower limit to the gas mass. Assuming optically thin emission and that the gas is in LTE, the total gas mass would be given by (e.g. Thi et al., 2001):

$$M_g \approx 10^{-4} (T_{\text{ex}} + 0.89) / e^{16.02/T_{\text{ex}}} I_{\text{CO}} \quad (1)$$

where T_{ex} is the excitation temperature, M_g the mass in units of Jupiter masses (M_J), the ¹²CO/H₂ abundance ratio is assumed to be 5×10^{-5} and I_{CO} is normalised to 100 pc

(see above). Most emission arises from the outer regions of these objects, where the dust kinetic temperature, T_{dust} , is between ~ 30 K (e.g. Beckwith & Sargent, 1993) and ~ 100 K (e.g. Dent et al., 2000). Assuming H₂ densities greater than 10^3cm^{-3} , then the gas and dust are sufficiently coupled for $T_{\text{dust}} \approx T_{\text{ex}}$. From eqn. (1), the likely range of temperatures will affect the derived mass limit by no more than a factor of 2 and so, adopting an excitation temperature of 60K, the horizontal line at $I_{\text{CO}} = 0.1$ on Fig. 1 corresponds to a minimum mass of $10^{-3} M_J$.

Also included in Fig. 1 are published limits to the J=2-1 CO emission from the Vega-excess stars Vega, β Pic, Fomalhaut and HR4796 (Dent et al., 1995; Liseau, 1999); we have assumed the same brightness temperature limits in both the J=3-2 and J=2-1 transitions.

The plot shows a clear link between the detectability of CO and a high fractional excess. We find 18 of the 27 objects with $f \geq 0.1$ are detected (upper right of the figure). Including the upper limits, the results indicate that 67 - 100 per cent of objects with $f > 0.1$ and 56 - 98 per cent of objects with $f > 0.01$ have significant CO emission (defined as where $I_{\text{CO}} \cdot (D/100\text{pc})^2 \geq 0.1 \text{Kkms}^{-1}$). The remaining stars with $f < 0.01$ are generally not detected in CO (only 2 or possibly 3 clear detections out of 27 objects with uncontaminated spectra). Ignoring the three very distant objects with poor scaled upper limits, this implies that $\sim 8 - 20$ per cent of low-excess objects ($f < 0.01$) have $I_{\text{CO}} \cdot (D/100\text{pc})^2 \geq 0.2 \text{Kkms}^{-1}$. However there are some notable exceptions to this general rule which are worth looking at individually.

HD98800 is the only star with $f \geq 0.01$ where the CO limit is significantly lower (ie $\geq 3\sigma$) than all the others. As will be shown later, this indicates a relatively small limit to the surface area of circumstellar gas, although it may be linked to the fact that this is a quadruple system. Conversely, there are two (possibly three) discs with low f (< 0.01) which have relatively bright CO emission: HD141569, which has a clear double-peaked line and a scattered light disc, HD9672 (also double-peaked) and HD4881. These will be discussed individually in later sections.

For a reprocessing disc viewed near face-on, the infrared excess is approximately the fraction of stellar radiation intercepted by the disc. To first order this is the effective solid angle subtended by the disc as seen from the star so, assuming a disc of constant opening angle θ , and mean optical depth through the disc to optical stellar photons of τ_V , the excess f is given by (e.g. Backman & Paresce, 1993):

$$f = (1 - e^{-\tau_V}) \sin(\theta/2) \quad (2)$$

In a typical photodissociation region, CO can survive at $A_V \geq 2-6$ (Hollenbach et al., 1991). As $\tau_V \sim A_V$, then assuming that photons from the central star are the dominant cause of CO dissociation (van Zadelhoff et al., 2003), we can estimate the disc opening angle required for significant CO to be present. The results of this survey imply that > 67 per cent of discs of opening angle $\geq 12^\circ$ ($f \geq 0.1$) will have gas masses $\geq 10^{-3} M_J$. Including the upper limits and ignoring the quadruple system HD98800, the results are consistent with *all* discs of $f \geq 0.01$, or $\theta \geq 1^\circ$, having at least $10^{-3} M_J$ of molecular gas.

The low extinction along the line of sight towards the stars with detected circumstellar CO (typically $A_V \sim 1$ mag;

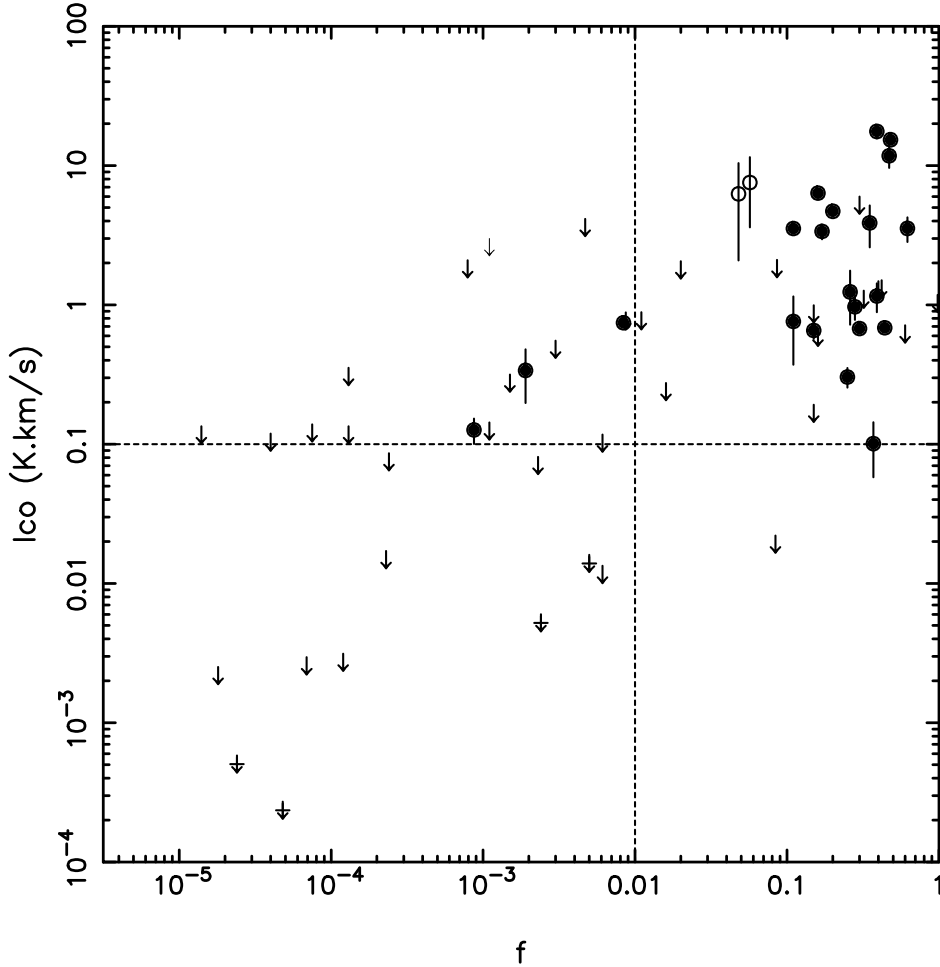


Figure 1. Integrated CO intensity for target stars ($T_{\text{mb}}dv$, in units of K km s^{-1}) normalised to a distance of 100 pc, plotted against the fractional excess of continuum emission above that of the stellar photosphere. Objects with clear CO detections are depicted as filled circles and those with uncertain identifications as open circles; the $1\text{-}\sigma$ upper limits of the remainder are also shown. Also included are published CO upper limits of nearby archetypal Vega excess stars (Dent et al., 1995; Liseau, 1999); these are shown as upper limits with a cross. The horizontal dashed line represents a minimum gas mass of $10^{-3}M_{\text{J}}$, and vertical line represents the critical excess for CO emission (see text for details).

van den Ancker et al., 1998) means we are unlikely to be looking through the disc itself, so the inclination $i < (90 - \theta/2)$. Assuming the sample of discs is randomly-oriented on the sky, the mean inclination would be 60° , giving a mean opening angle θ of $< 30^\circ$. For realistic discs, the photons may be intercepted at an inner hot bulge (e.g. Natta et al., 2001) rather than an outer flaring region, although either structure would result in an increase in the total excess f , as well as shielding more distant gas in the disc from UV photodissociation; as a result the above relation would still apply.

The gas discs with the lowest f are HD141569, HD4881 and HD9672; from eqn. 1, their opening angles range from $\sim 1^\circ$ down to as small as 0.1° . There is no evidence for strong near-infrared excesses in these stars (e.g. Sylvester et al., 1986) as predicted by the hot inner bulge models, which would suggest the optically thick regions of their discs have

relatively large radii as well as being physically thin. Such structures are even thinner than the opening angle of 7° seen in the edge-on β Pictoris dust disc (Heap et al., 2000), and the detections of CO imply it can also exist in such thin layers.

4 SPECTRAL PROFILES

Emission from CO around five of the brightest isolated HAeBe stars have been resolved with interferometers (Mannings & Sargent, 1998, 2000; Piétu et al., 2003; Augereau et al., 2004). In all cases the material appears to be located in Keplerian discs with outer radii of a few hundred au; however the angular sizes are often only marginally larger than the existing interferometer beam sizes.

The CO emission intensity from most of the objects in

the current survey is $\leq 1\text{Kms}^{-1}$, and is difficult to image with existing interferometers. Consequently we have to rely on interpretation of the emission line profiles to derive kinematic and geometric information about the discs. It was noted by Beckwith & Sargent (1993) and others that low-J ^{12}CO lines in discs around young stars are likely to be optically thick, and so effectively trace the gas temperature on the disc surface rather than the total mass. A double-peaked line profile is a characteristic of such emission. Of the 21 stars with CO emission, 9 and possibly as many as 12 have clear double-peaked line profiles (Table 1). Formally a double-peaked profile can also arise from self-absorption in an extended cool outer envelopes (as found in obscured young stellar objects). However all our target stars have low optical extinction, suggesting that this effect is unlikely to be important.

A small number of objects (HD4881, HD143006 and UX Ori) have narrow lines ($\leq 1\text{km s}^{-1}$), consistent with emission from an ambient cloud. However, even in these cases the CO and stellar velocities are similar, suggesting the gas may be closely associated with the star. Four stars have single-peaked lines significantly broader than typical ambient gas emission; this is thought to be from a disc viewed close to edge-on (see below). The remaining lines have insufficient s:n to classify their shapes, although most are relatively broad. In the modelling described below, we have assumed all our detections are due to disc emission, and used the line profiles to estimate system parameters.

4.1 Modelling program

As recognised by, for example, Omodaka et al. (1992) and Beckwith & Sargent (1993), it is possible to derive some basic parameters of a disc, such as size and inclination, from fitting just the spectral profile of an optically thick tracer. The high mean density means the CO line is thermalised, allowing a simple model to be applied which assumes that the local excitation temperature is unaffected by emission from other parts of the disc. Significantly more complicated models of line emission from discs have been developed more recently which include the effects of chemistry, radiative transfer, different dust characteristics, more complex disc structures, and UV photodissociation (e.g. van Zadelhoff et al., 2001; Aikawa et al., 2002). However, each of these introduces many new uncertain parameters, and so in the absence of additional data for most targets, we have applied just a basic model to the J=3-2 CO profiles, minimising the χ^2 fit to the data.

The present model assumes the disc is in Keplerian rotation viewed at inclination i ($i=0$ implies a face-on geometry), with an effective opening angle, θ , at radius 100 au. Volume density in the mid-plane falls as r^{-3} , and the disc is flared, so the (Gaussian) scale height, z_0 , increases as $r^{1.5}$ (see Beckwith & Sargent, 1993). However, the CO profile is not sensitive to either of these power laws. The gas density n_{H_2} at radius r and height z above the disc plane, between R_{in} and R_{out} is then given by:

$$n_{\text{H}_2} = n_0(r/r_0)^{-3}e^{-(z/z_0)^2} \quad (3)$$

where the scale height is expressed as:

$$\left(\frac{z_0}{100\text{au}}\right) = \tan(\theta)\left(\frac{r}{100\text{au}}\right)^{1.5} \quad (4)$$

The density is assumed to be zero for $r < R_{in}$ and $r > R_{out}$. and n_0 and r_0 are scaling factors for the total disc mass, obtained from the dust mass assuming a constant gas:dust ratio of 100. Dust masses are obtained from the literature, mostly from fits to the continuum SED. The narrow features in several of the spectra suggests that the effect of turbulent line broadening is negligible; consequently only thermal broadening is included (see also Beckwith & Sargent; Piétu et al., 2003). The model assumes a constant gas:dust ratio without the effects of chemistry; Aikawa & Herbst (2001) indicate that chemical reactions in the disc do not significantly alter typical emergent lines profiles of molecules such as ^{12}CO , as the emission is so optically thick. However, the CO abundance can be affected by the local UV photoionisation rate, which depends on distance and extinction to the star and the stellar spectral type, as well as the interstellar radiation field and optical depth to the surface of the disc. The stellar photodissociation is based on an analytical fit to the model of Hollenbach et al. (1991). Interstellar photodissociation is approximated by effectively removing emission from the disc surface down to $A_V = 3$ mag. However, in most cases the density is sufficiently high that the UV has little effect on the CO abundance throughout most of the disc volume.

As the mean densities for most discs under investigation are typically $\gg 10^4\text{cm}^{-3}$, then the gas and dust will be in thermal equilibrium; the dust temperature is assumed to be that of small grains radiatively heated the star (e.g. Aikawa & Herbst, 2001). The excitation temperature is then given by:

$$T_{ex} = 282.\left(\frac{L}{L_\odot}\right)^{0.2}.\left(\frac{d}{\text{au}}\right)^{-0.4}.\left(\frac{a}{\mu\text{m}}\right)^{-0.2} \quad (5)$$

Smaller grains, such as classical ISM dust, will be hotter, but offsetting this is the possibility that the outer disc may be shielded from the star by the inner regions and so would be cooler. The extinction to the star depends on the flaring angle and detailed structure of the inner disc; for a flared disc for example, the dust higher above the disc plane will be hotter. The effective CO excitation temperature at a particular radius is approximately that at the ‘ $\tau=1$ ’ surface (van Zadelhoff et al., 2001). The height of this surface above the disc plane depends on θ and the inclination angle i as well as the disc structure. In the case of a face-on disc, comparison of the temperatures at the $\tau=1$ surface (see van Zadelhoff et al., 2001, their Figure 6) with the temperatures assumed in our present model indicates that we may be underestimating the temperature at a given radius by a factor of between 1.0 and 2.0. For more inclined discs, however, we will see deeper into the gas, and so the temperature at the ‘ $\tau=1$ ’ surface will actually be lower. This suggests that the uncertainty in T_{ex} is less than a factor of 2; for unresolved discs in an optically thick line, this implies the disc radius would then be in error by a factor of ≤ 1.5 , which gives some indication of the possible uncertainty of R_{out} .

4.2 Line profile fitting

The spectra of the targets with significant detections of CO are shown in Figure 2, along with the best fit models. Table 2 summarises the modelling results for these objects; also given is the derived disc angular diameter. In some cases the

parameters are not well constrained because of the low s:n of the data - this is indicated in the table. Dust masses marked (1) are scaled to the adopted distances. Lines with a clear double-peaked profile are identified by ‘D’.

In most cases, the CO profiles can be fitted reasonably well by the simple disc model by a suitable choice of i and R_{out} . As the line emission is generally optically thick from all regions of the disc, the disc outer radius determines the intensity to first order, and the disc inclination mainly affects the overall line width. The inner radius is constrained by the line wings although, apart from the closest objects, beam dilution of emission from this compact region means R_{in} is not well constrained. The opening angle θ has a small effect on the line intensity and shape at the lower relative velocities, although in most cases we cannot constrain it, and have simply set it to a fixed value.

The spectra from nine objects listed in Table 2 have clear double-peaked spectra consistent with a disc. Another nine objects have single-peaked lines, although only a small number of these (HD4881, HD143006 and UX Ori) have narrow line widths more consistent with ambient cloud emission ($< 1 \text{ km s}^{-1}$). The remaining have more ambiguous line profiles (CQ Tau, HD139614, HD144432, HD145718), although all are relatively broad suggesting they arise from a disc rather than an ambient cloud. Apart from HD179218 and HD233517 the stellar velocities, if known, agree with those of the CO, confirming the gas is associated with the stars. Assuming all the single-peaked profiles arise from discs viewed almost face-on, then the average outer radii of these objects is 110 au, compared with 170 au for the double-peaked and broad spectra; the similarity of these values also suggests a common origin for all emission. In the following sections, we discuss the results for individual objects.

4.2.1 HD9672

HD9672 (49 Cet) is one of only three debris discs with $f > 10^{-3}$ (e.g. Jayawardhana et al., 2001), the other two being HR4796 and β Pictoris. A weak CO line was detected by Zuckerman et al. (1995), making this not only the only bona-fide debris disc with detectable CO, but also one of the closest gas-rich discs (only TW Hya is closer). Fig. 2a confirms the emission centroid lies close to the stellar velocity (9.86 km s^{-1}) and shows the line profile to be double-peaked.

Weinberger et al. (1999) saw no evidence of scattered light at radii beyond 1.6 arcsec (~ 100 au), although Jayawardhana et al. (2001) did detect mid-infrared emission extending to a radius of ~ 50 au. The relatively weak CO line brightness implies the emission region likely has a small surface area. The data are consistent with a compact disc (outer radius ~ 17 au) inclined at 16° . The relatively high velocity wings imply gas is present at radii ≤ 5 au. A more inclined ring ($i \sim 35^\circ$) of radius 50 au (equal to that seen in the mid-infrared) would produce a similar separation of the line peaks but does not reproduce the higher velocity wings (see dashed line on the spectrum in Fig. 2a).

4.2.2 AB Aur

A disc was resolved around this star using mm-wave interferometry in the J=1-0 ^{13}CO line (Mannings & Sargent,

1997). The beam size was 4-5 arcsec (~ 720 au) and the derived outer radius was 450 au. HST images show a scattering disc extending to a radius of ~ 8 arcsec (Grady et al., 1999), and an extended arc of dust at $r \sim 10 - 20$ arcsec, likely due to remnant ambient gas. Grady et al. suggest that the disc is almost face-on ($i < 45^\circ$), and may be flared, judging by the radial emission profile.

Our fit using an outer radius of 600 au (Fig. 2a) shows reasonable agreement with the spectrum at low relative velocities. Notably, the narrow linewidth implies that the disc must be almost face-on ($i \sim 12^\circ$), agreeing with the symmetrical optical image, rather than the higher inclination derived from the interferometer map. But this simple model cannot explain the line wings seen out to relative velocities of $\pm 2 \text{ km s}^{-1}$. This implies that either the inclination of the inner region of the disc is higher (a model with $i = 17^\circ$, $i \sim 300$ au can fit the profile of the wings alone, and is shown by the dashed line in Fig. 2a), the low-velocity emission is dominated by ambient gas, or there is an additional higher-velocity component such as a molecular outflow. The presence of highly extended, possibly ambient material in the scattered light images suggests that the narrow central component in the ^{12}CO line may not be from the disc itself; consequently $i = 17^\circ$ and $R_{out} \sim 300$ au may represent the true values of the circumstellar disc.

4.2.3 MWC480

This disc has been resolved in J=2-1 CO using interferometry with a 1.8 arcsec beam (Mannings et al., 1997). By comparing with a two-component Gaussian model of surface brightness, they derived an outer cutoff of ~ 650 au (after scaling to the distance in Table 1). However, our data (Fig. 2a) are consistent with a disc model with outer radius ~ 245 au; the reason for this discrepancy is thought to be differences in the model and possibly the increased sensitivity of their J=2-1 data to extended lower-density extended regions.

In addition to the double-peaked shape, two other features in the deep CO spectrum are worthy of note. One is that emission is detected out to relative velocities of $\pm 3.5 \text{ km s}^{-1}$, implying the gas disc has an inner radius smaller than 20 au. The second is that the line profile is clearly asymmetrical; a similar asymmetry was seen in the reconstructed interferometric spectrum of J=2-1 ^{12}CO in Mannings et al. and the ^{13}CO single-dish spectrum in Thi et al. (2004), although the s:n of both of these spectra are lower than shown in Fig. 2a. A possible explanation is that the asymmetry is due to systematic telescope pointing offsets. With a 14 arcsec Gaussian beam, the observed 30 per cent difference in intensities of the two peaks in Fig. 2a would require a consistent pointing offset of 5 arcsec along the disc plane. Not only is this significantly larger than normal telescope pointing errors, but also the data were taken from runs on several different nights with consistent results. We have instead attempted to fit this asymmetry by imposing a sinusoidal azimuthal deviation in either the density or temperature around the disc. As the CO emission is optically thick over most of the disc, implausibly large deviations in density of ≥ 99 per cent are necessary to explain the asymmetric spectra. However, the peak-to-peak temperature difference required to match the line profile is 30 per cent. The ori-

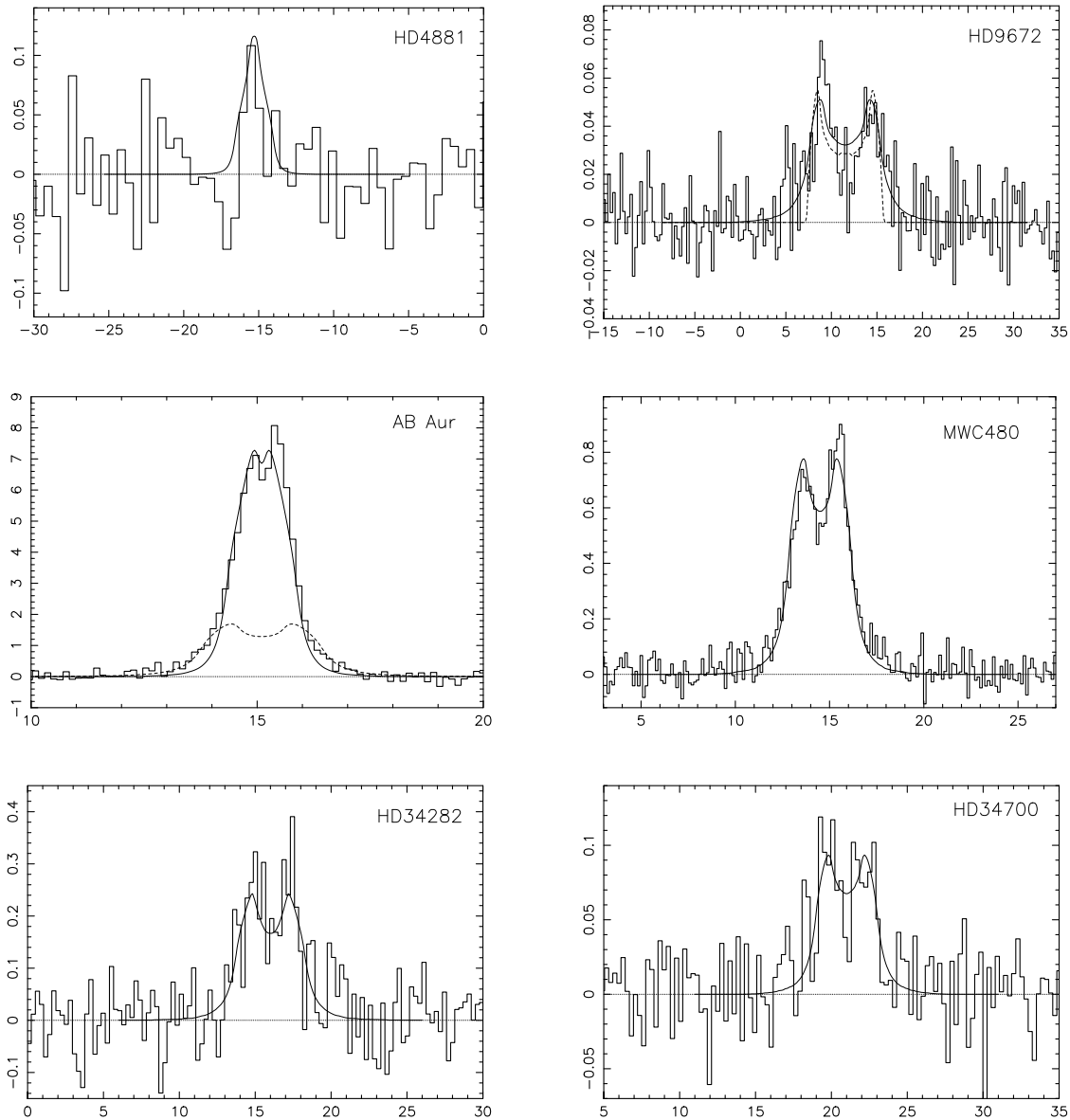


Figure 2. (a-d) Spectra of $J=3-2$ ^{12}CO for the objects where emission was detected (histogram). Also shown are the best fit models (solid line); in some cases an alternative model is shown by the dashed lines - see discussion of individual objects for details. Model parameters are given in Table 2 and described in more detail in the text for individual objects. Velocity scale is km s^{-1} (Heliocentric reference), and intensity unit is main beam brightness temperature (K); note that the ranges on the axes vary from source to source.

gin of such a putative temperature difference could be non-axisymmetric variations in the disc structure; for example one sector may be more flared and exposed to the stellar radiation.

This asymmetry needs further confirmation with high $s:n$ data in other molecular lines, along with more detailed modelling including a fuller treatment of dust temperature and structure throughout the disc.

4.2.4 *HD34282*

A detailed model has been derived from interferometric data by Piétu et al. (2003), including a revision to the distance and hence the luminosity of this star (see Table 1). The results from fitting our single-dish spectrum give an inclination consistent with their data, although the outer radius from our fitting is 360 au, a factor of ~ 2 smaller than theirs. The peak line brightness in Fig. 2a is 0.3K; if the disc is optically thick with a mean brightness temperature of 30K, this would suggest a beam filling factor of 1 per cent and hence a radius of $\sim 300\text{au}$, more consistent with the current model.

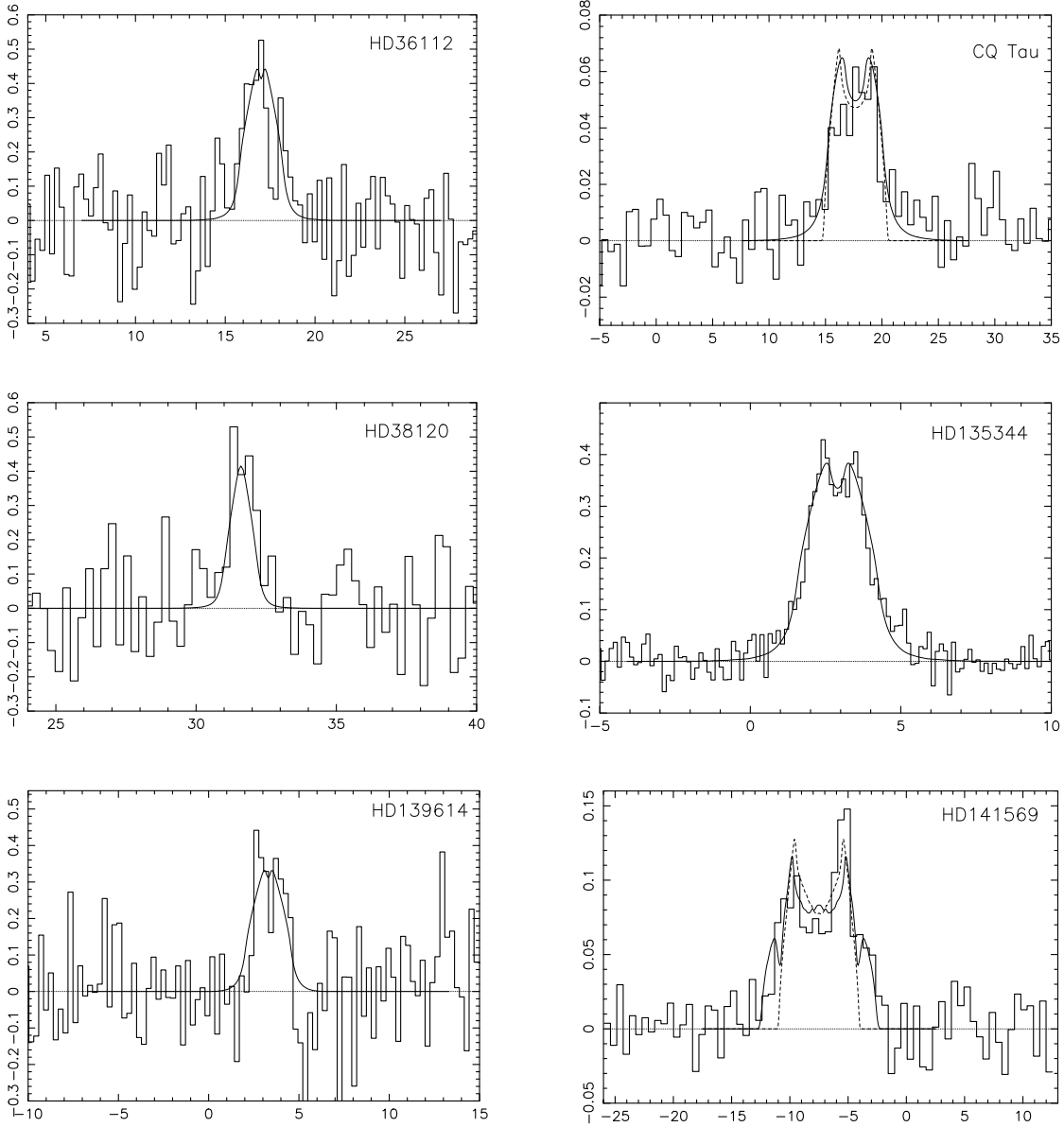
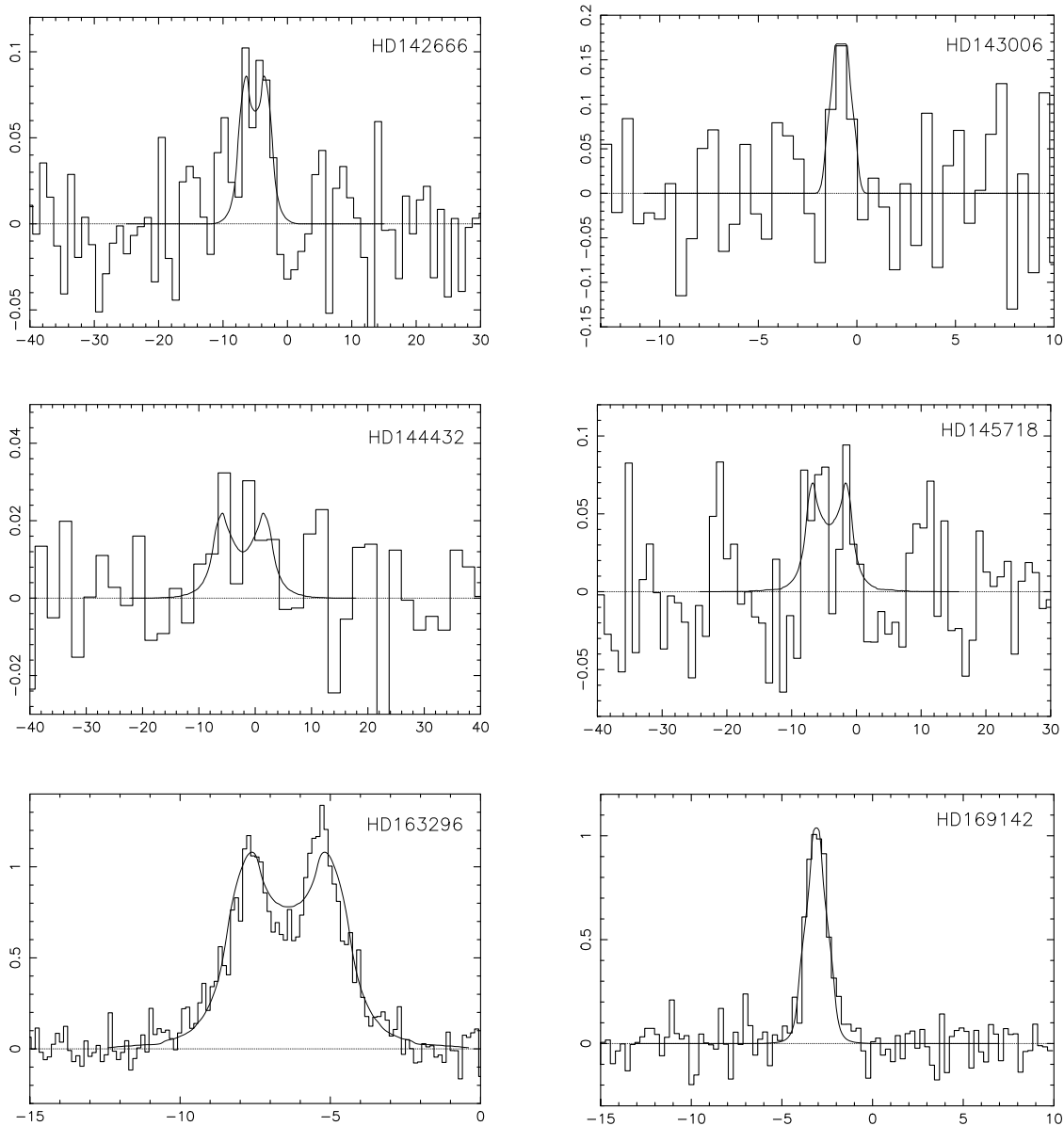


Figure 2. (b)

4.2.5 CQ Tau

This object is thought to be a UX Ori star, suggesting the disc is viewed close to edge-on, and an inclination of 66° was estimated based on a model of the variability by Natta & Whitney (2000). An upper limit to the gaseous disc radius of 85 au was measured using interferometry (Mannings & Sargent, 2000), although Testi et al. (2003) resolved the dust continuum emission at 7mm, finding a radius of 100-200 au. The single-dish CO spectrum shows a relatively broad but weak line (Fig. 2b), which can be fitted with a contiguous disc of outer radius 30 au (inner radius ≤ 10 au) and inclination 14° (the solid line in the figure). But this inclination is inconsistent with previous estimates based on the variability. A larger, thin and somewhat more inclined ring model would fit the observed brightness temperature and width of

the line core, and be consistent with the maximum dust radius ($R_{out} = 80$ au, $R_{in} = 70$ au, $i = 30^\circ$, $\theta = 2^\circ$; see dashed line in Fig. 2b). However, there is weak evidence of broad line wings, which are not reproduced by such a thin ring; furthermore a ring with an inclination as high as 66° would be inconsistent with the narrow CO line and compact size from interferometry. To reconcile this difference, the system could contain a compact gas disc or ring with low inclination, but with a highly flared dust disc; alternatively the gas lies in a more extended ring, but the line brightness is low because of CO depletion and excitation conditions in the disc atmosphere, which have not been included in the present model.

**Figure 2.** (c)

4.2.6 HD135344

This is the one of the closest gas-rich discs to the Sun (CWD98), and also the oldest known star with such a disc: Thi et al. (2001) derive an age of 16.7 Myr. No scattered light has been detected using coronagraph observations down to radii of ~ 1 arcsec although a binary pair was found at separation ~ 5.8 arcsec (490 au) from the primary (Augereau et al., 2001). The CO line is double-peaked (Fig. 2b) and can be well fitted by a compact disc of outer radius 75 au viewed nearly face-on. A more extended edge-on ring is excluded by the presence of wings in the line profile. If we assume the nearby binary pair are associated with HD135344, this would imply an upper limit of ~ 200 au to the disc radius, as

material is unlikely to exist in a stable orbit at radii within a factor of ~ 2 of the binary separation.

4.2.7 HD141569

An extended region of scattered light from a circumstellar disc has been imaged by several authors using coronagraphy (e.g. Mouillet et al., 2001, and refs. therein), and both this and mid-infrared images indicate an inclination of 52° . In addition, CO emission was detected from this object by Zuckerman et al. (1995), and recently imaged using interferometry (Augereau et al., 2004). We obtained a deep CO spectrum (Fig. 2b), which shows a double-peaked line profile, with a distinctive “shoulder” at higher relative velocities. A single ring or disc structure cannot explain this line-

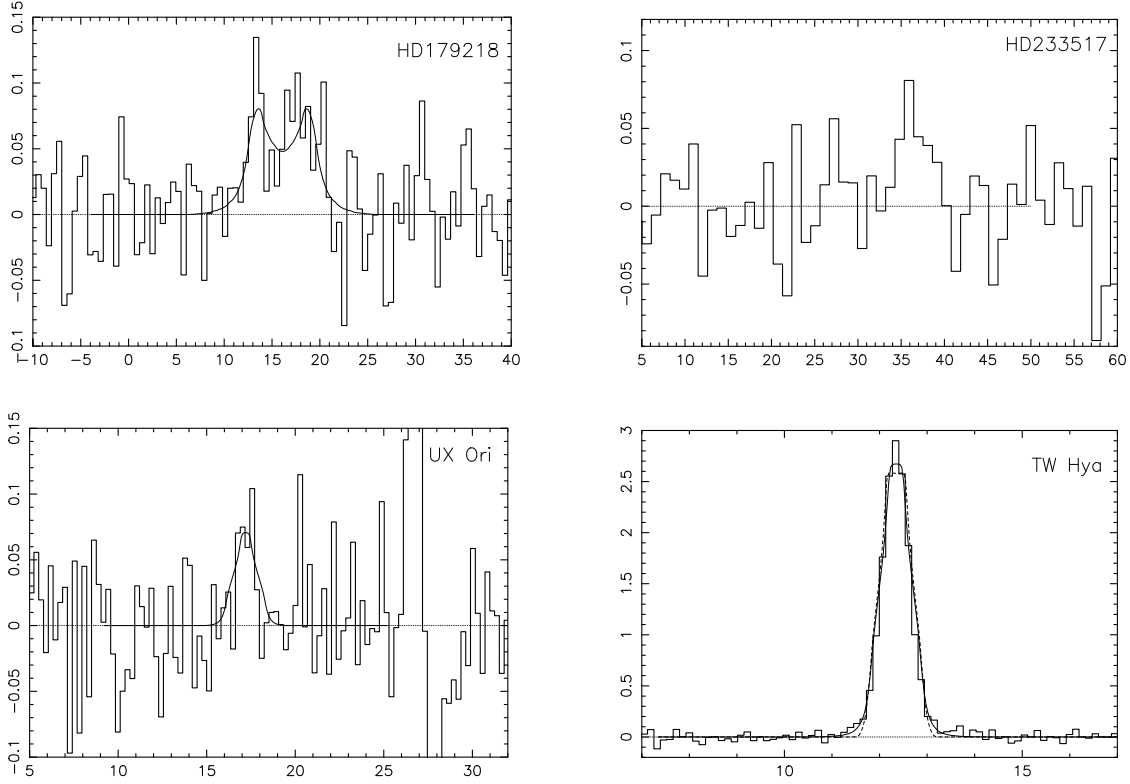


Figure 2. (d)

Table 2. Stars with CO detections: best fit model parameters.

Star	Dust mass (M_{\odot})	R_{in} (au)	R_{out} (au)	D_{out} (arcsec)	i	θ	Notes ⁽²⁾
HD4881	3.9×10^{-5}	-	35	0.4	≤ 5	≤ 10	
HD9672	4×10^{-6}	< 5	17 ± 5	0.6	16 ± 3	10	D
AB Aur	2.1×10^{-4}	≤ 50	600 ± 50	8.4	12 ± 2	5	D; Poss. 300au inner disc - see text
MWC480	2.0×10^{-4}	≤ 20	245 ± 30	3.8	28 ± 2	10	D
HD34282	1.1×10^{-3}	≤ 50	380 ± 20	1.8	50 ± 5	10	D
HD34700	$2.1 \times 10^{-5(1)}$	≤ 30	80 ± 10	1.3	25 ± 2	10	D
HD36112	2.9×10^{-4}	-	170 ± 30	1.7	≤ 10	10	Single broad line
CQ Tau	2.2×10^{-4}	≤ 10	30 ± 5	0.7	14	10	Broad line
HD38120	10^{-5}	-	300 ± 50	1.2	< 8	10	
HD135344	10^{-4}	≤ 10	75 ± 5	1.8	11 ± 2	10	D
HD139614	10^{-4}	≤ 20	110 ± 3	1.4	≤ 10	10	
HD141569	10^{-5}	90 ± 5	250 ± 2	5.0	52	0.5	D; Double ring structure - see text
HD142666	3×10^{-4}	-	45 ± 10	0.8	18 ± 5	10	Single broad line
HD143006	1.6×10^{-5}	-	35 ± 5	0.8	≤ 3	10	
HD144432	2×10^{-3}	-	60 ± 20	0.6	48 ± 10	10	Low s:n; broad line?
HD145718	4.5×10^{-5}	-	60 ± 30	0.9	32 ± 10	10	Low s:n
HD163296	5×10^{-4}	≤ 20	245 ± 20	4.0	30 ± 2	≤ 10	D
HD169142	10^{-3}	-	130 ± 10	1.8	≤ 5	10	
HD179218	10^{-4}	-	120 ± 20	1.9	40 ± 10	10	D; Stellar and CO velocity differ
HD233517	$1.7 \times 10^{-4(1)}$	-	-	-	-	-	Stellar and CO velocity differ
UX Ori	4.2×10^{-4}	-	95	0.4	≤ 8	10	Additional ambient gas component
TW Hya	3.0×10^{-4}	≤ 30	160 ± 10	5.7	5 ± 2	≤ 10	

shape, giving for example, the model shown by the dashed line in Fig. 2b. Instead we adopted a double ring structure. The inclination of the dust disc is well constrained by the images so we adopt the same value for the gas. The relatively narrow overall line width indicates ring radii of 95 and ~ 250 au (shown by the solid line on Fig. 2b). The latter is similar to the radius found in the recent interferometry results. The low disc mass and high UV luminosity of the star requires the rings to be physically thin in order to maintain high extinction and avoid photodissociating the CO. The best fit to the data has an opening angle $\theta = 1.0^\circ$, consistent with the low fractional infrared excess of the star (see Table 1). The low observed CO brightness temperature implies the surface area, and therefore the radial extent of the rings, must also be small. In order to fit the intensities, radial widths of ~ 20 au and 8 au are required for the inner and outer rings.

The dust rings seen in scattered light reach peak densities at radii ~ 200 and ~ 350 au (Mouillet et al.). The gaps detected in dust extends from $\leq 125 - 175$ au (measurement of the inner radius was limited by the coronagraph occulting bar) and 215 - 300 au. Our CO model suggests emission also arises from a ring inside this, at radius 90 au, similar to the size of the mid-infrared source (Fisher et al., 2000). Brittain et al. (2003) also detected near-infrared ro-vibrational CO lines from the disc; the linewidths and temperatures indicate that this arises at radii 17 - 50 au, which may correspond with the innermost edge of our inner CO ring.

A further feature of the spectrum in Fig. 2b is the asymmetry of the narrow component; at positive velocities the line is ~ 50 per cent brighter than at negative velocities. As noted for MWC480 above, if the CO emission is optically thick, this would require a large variation in density within the ring (or a smaller variation in temperature). In the case of HD141569, a large variation in CO density could be explained by a difference in the extinction to the star (and hence differences in photodissociation rate). A recent K-band image (Boccaletti et al., 2003) also shows an asymmetry in scattered light, whereby the north-eastern sector of the 200 au ring is significantly brighter. If this is related to the CO asymmetry, it would indicate this is the side of the ring approaching us.

Overall the CO model of HD141569 suggests that molecular gas and dust is well intermixed in a physically thin pair of rings. A more detailed comparison between the scattering dust and molecular gas would require a high resolution CO map of this complex system.

4.2.8 HD163296

The disc around this star has been resolved both in scattered light and mm-wave interferometry (Mannings & Sargent, 1997; Grady et al., 2000). Our high s:n spectrum shows reasonable agreement with a model disc inclined at 30° (Fig. 2c), although the deep dip near the stellar systemic velocity cannot be reproduced in a simple model. One possible explanation for this might be self-absorption from cool foreground gas, although the low optical extinction to the star suggests little material exists along the line of sight (van den Ancker et al., 1998). The CO spectra of Thi et al. (2004) shows line-of-sight gas at velocities considerably different from that of the star (and outside the range shown

in Fig. 2c); however, there is no evidence of extended emission at the stellar velocity itself. The derived disc inclination is inconsistent with that found from the morphology of the interferometric map - we cannot reproduce the line profile with inclinations as high as 60° . However, the derived outer radius is in close agreement with the interferometric result, and is similar to the inner edge of the dark lane seen in scattered light, indicating that the gas and dust co-exist within the disc. Modelling the CO emission profile out to relative velocities of $\pm 4 \text{ km s}^{-1}$ suggests that gas exists in the disc down to radii less than 20 au. No additional high-velocity molecular outflow component is needed to explain the line shape.

4.2.9 UX Ori

Extended CO emission is seen in this region at $v \sim 27 \text{ km s}^{-1}$ in both the signal and reference positions, however, a narrow emission line was also seen at the stellar velocity itself (Fig. 2d). All model fits which assume the emission is from a disc require an orientation close to face-on ($i \leq 20^\circ$) to reproduce the line width. This is inconsistent with the interpretation of the variability as obscuration in a near edge-on disc (Natta et al., 1999). The line may instead be from ambient gas more distant from the star, possibly associated with the extended far-infrared emission seen by Natta et al.; mapping of this emission would help identify its origin.

4.2.10 TW Hya

We obtained a deep CO spectrum of disc around the 8 Myr old star TW Hya, known to have numerous emission lines at sub-mm wavelengths (e.g. van Zadelhoff et al., 2001). Although TW Hya is a K7 rather than an AeBe star, the disc is well known to be close to face-on; we have included it in this study partly to compare the results from our simple LTE model with the more detailed radiative transfer and chemistry modelling carried out by van Zadelhoff et al., and partly to search for weak higher-velocity gas in the deep spectrum. Assuming standard ^{12}CO abundance, we derive a disc outer radius of 160 au, very similar to the scattered light images, as well as the size derived from the SED (Calvet et al., 2002) and that adopted by van Zadelhoff et al. Furthermore the CO abundance depletions measured by van Zadelhoff et al. (up to 150) do not significantly affect the derived result; for such a depletion, the disc size required to fit the present data increases only slightly (190 au), confirming that the emission is indeed extremely optically thick.

The narrow line width seen in Fig. 2d indicates an inclination of only $i \sim 5^\circ$ and a physically thin disc ($\theta \sim 5^\circ$). However, weak wings reaching to $\pm 1.3 \text{ km s}^{-1}$ can be seen in the deep spectrum. These require a model where the gas disc extends in to a radius ≤ 30 au (for comparison, a model with a central hole of radius 50 au gives the spectrum shown by the dashed line). This compares with the innermost edge of the dust disc and the developing gap (4 au) derived by Calvet et al. from the continuum SED.

5 DISCUSSION

5.1 Disc outer radii

The outer disc radii derived in our sample of stars mostly lie between 30 and 400 au, with a mean of ~ 150 au. Most are larger than the solar system (~ 50 au to the edge of the Kuiper Belt), and are closer to the size of the debris discs seen around older stars (typically 50 - 150 au, e.g. Holland et al., 1998). However, as many as 5 of the gas discs are compact ($R_{out} \leq 50$ au), and at least another 7 have evidence of gas at inner radii smaller than 50 au. So what determines the radius, and how is the gas removed?

Figure 3 shows that the disc size is not correlated with the stellar spectral type, with a Pearson correlation coefficient of -0.04. This applies over 2.5 orders of magnitude in luminosity. We also include published T Tauri disc radii from Simon et al. (2000) as well as model fits to the CO upper limits for stars in Table 1 with $f \geq 0.1$, ie which are predicted to have measurable CO emission (see discussion above).

Figure 3 also shows the radius at which a black body in thermal equilibrium with the central star reaches the CO freeze-out temperature (assumed to be 20K). This assumption of black body temperature would require large grain sizes ($> 1mm$), as well as low extinction to the star. It is likely that the disc mid-plane temperature would be lower than this in some objects due to the high extinction. Conversely, if the grain sizes were closer to those in the interstellar medium (ie little grain growth had occurred) the temperature would be higher. If freeze-out were important, we would not expect to see disc radii above this line. Fig. 3 shows that this is indeed the case for all stars of type F or earlier. However, some T Tauri stars lie above this line, suggesting that another source of energy such as accretion luminosity may be heating these discs.

5.2 Comparison with dust discs

The continuum SEDs from many of the objects in Table 2 have been used to derive disc sizes, based on standard dust models (e.g. Dominik et al., 2003). In all cases except HD135344, the SED-derived radii are smaller than those derived from CO; we attribute this to the greater sensitivity of the J=3-2 transition of CO to a given mass of material. However, it is possible that large grains could accrete rapidly through a disc, leaving a gas disc larger than the dust disc (Takeuchi & Lin, 2002).

We can also compare the total disc mass (derived from the continuum SED, scaled assuming a constant gas:dust ratio of 100) with the gas disc outer radius (Fig. 4). There is some evidence of a correlation between the disc size and mass, with a Pearson correlation coefficient of 0.62. The slope of the fit is 2.8, close to a value of 3 which would apply if the mean density in the discs was constant. Further data over a wider range of masses would be needed to confirm this result.

Scattered light from dust around four discs in Table 2 has been detected using coronagraphy (AB Aur, HD141569, HD163296 and TW Hya). These are all predicted from the CO modelling to have angular sizes > 3 arcsec. Their optical sizes and distributions are similar to those derived from CO,

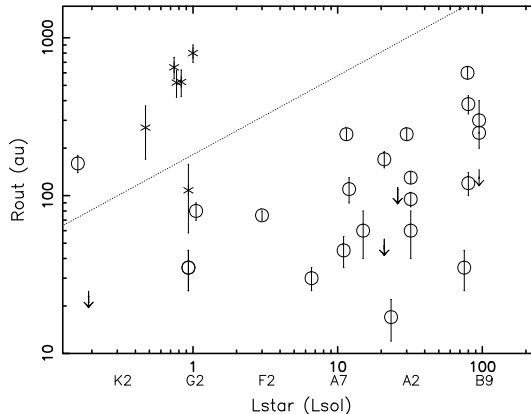


Figure 3. Derived outer radii of gas disc plotted as a function of stellar luminosity and Zero Age Main Sequence spectral type. The straight line shows the temperature at which CO freezes out onto grains (see text). Also shown are derived upper limits (2σ) to the disc size for stars with no line detection, but which have $f \geq 0.1$. The star symbols represent the interferometric observations of discs around T Tauri stars from Simon et al. (2000).

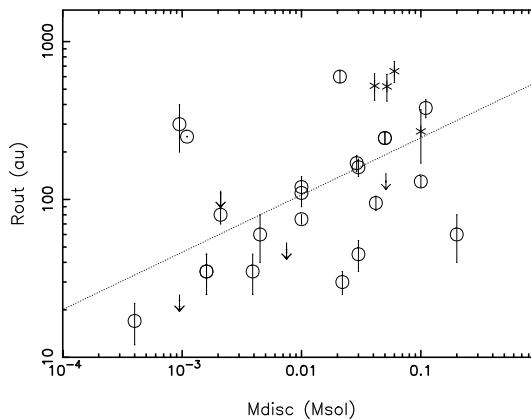


Figure 4. Derived outer radii of gas discs plotted as a function of disc mass from dust continuum fluxes. Disc mass includes the gas, assuming a constant gas:dust ratio of 100. The upper limits to the sizes represent stars in the present survey with $f \geq 0.1$. The star symbols represent the interferometric observations of discs around isolated T Tauri stars from Simon et al. (2000). The line is a fit to the data, with a slope of 2.8.

implying that the gas and small scattering dust grains are closely intermixed. The predicted angular size of MWC480 also suggests that scattered light may be detectable, however, coronagraph imaging has not shown extended emission (Augureau et al., 2001). One possible explanation is that this disc is not flared, or is shadowed by a thick inner disc.

5.3 Gas disc lifetimes

Many authors have used disc masses derived from mm-wavelength continuum or line fluxes to estimate the disc lifetime (e.g. Beckwith et al., 1990; Thi et al., 2001), and the results suggest that dust discs survive for typically $\sim 10^7$ yr. However, mass estimates are uncertain because the detectable dust is part of a broad grain size distribution and so represents only a small fraction of the total solid mass. The gas:dust ratio is also uncertain (e.g. Thi et al., 2001), and is likely to evolve in these discs. Rather surprisingly, the results show no evidence of evolution of disc *mass* between ages of 10^5 and 10^7 yr, around either T Tauri (Beckwith et al., 1990) or HAeBe stars (Natta et al., 2000).

Although we cannot derive gas masses from ^{12}CO (see above), we can use the results to see whether there is an evolution in *size* of the gas disc; this is illustrated in Figure 5. Typical uncertainties in the age derivations are 1-3 Myr, and dominate the plot. However, splitting the sample in two based on their age, the discs around older objects (7-20 Myr) have a mean radius of 75 au, significantly smaller than the younger discs (3-7 Myr), where the mean radius is 210 au. There are no large, old gas discs (which would appear in the top right of the figure). This effect is strengthened further if the published results from relatively young (1-5 Myr) T Tauri discs are included. Although these have significantly lower luminosity, the lack of dependence of size with spectral type (see Fig. 3) indicates that disc age is more important than stellar luminosity. Discs around even younger stars (Class I or II YSOs, typically of age 0.1-1 Myr) are difficult to separate from surrounding ambient clouds, both observationally and in the definition of where the disc ends and “ambient” gas begins. Fuente et al. (2002) found that the very large-scale ($\geq 10^4$ au) ambient gas around HAeBe stars disappears by ~ 1 Myr. However interferometric observations show discs with radii of a few 10^2 to $\sim 10^3$ au around some Class I stars, thought to be ≤ 1 Myr in age (e.g. Mundy et al., 2000). Overall Fig. 5 shows evidence for evolution of the gas disc size, such that R_{out} decreases by a factor of ~ 3 over the 3-20 Myr period. An alternative view is that the lifetime of the outer ~ 200 au gas disc region is ~ 7 Myr, and the inner ~ 75 au region is ~ 20 Myr. However, this result should be treated with caution, as the age determinations are somewhat uncertain.

Models of disc removal suggest that timescales should *increase* with radius (e.g. Hollenbach et al., 2000). So we might expect relatively little evolution of the outer radius except at the end of the disc lifetime, when the gas rapidly disappears (Clarke et al., 2002) or the obscuring dust coagulates, allowing photodissociation of the outer regions. However, the dominant removal mechanism in the outer (100-1000 au) region of the disc may be external photoevaporation (Matsuyama et al., 2003) or interaction with other stars in a young cluster (Mundy et al., 2000). The decrease in mean outer radius in Fig. 5 would therefore be determined

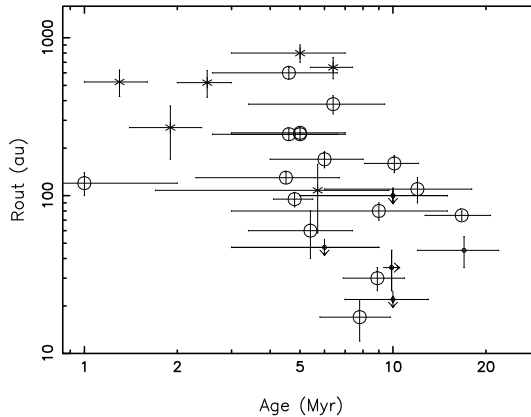


Figure 5. Derived outer radii of gas discs plotted as a function of stellar age. Large circles represent stars whose ages are well-determined using stellar evolutionary tracks; smaller circles represent stars where the age is more uncertain. Ages are taken from Zuckerman et al (1995), Natta et al. (1997), Thi et al. (2001), van den Ancker et al. (1998), Dominik et al (2003) and Natta et al. (2004). The upper limits to the sizes represent stars in the present survey with $f \geq 0.1$ which have known ages. The star symbols represent the interferometric observations of discs around isolated T Tauri stars from Simon et al. (2000).

by interaction with the local environment, rather than evolution of the star itself.

Finally the results of the modelling indicate that at least 10^{21} kg of gaseous CO exists for ~ 20 Myr at radii ≤ 100 au around these stars. This could be available to form $\sim 10^9$ 1 km-sized comets, assuming a cometary CO mass fraction of 10 per cent.

6 CONCLUSIONS

We have surveyed a sample of 59 isolated HAeBe stars and Vega-excess stars for sub-mm ^{12}CO emission. A clear correlation with fractional excess is seen, with a high CO detection rate around stars with $f \geq 0.1$ (18/27) and a low detection rate for those with $f < 0.01$ (2/27). This is explainable by CO dissociation by stellar UV photons; the stars showing high f have an optically thick disc shielding the gas. Most discs with detected CO have derived opening angles $\geq 12^\circ$, although in the low- f objects, the shielding disc must be geometrically thin ($\theta < 1^\circ$). The data are consistent with *all* of the $f > 0.1$ discs having significant gas (with a minimum mass of $10^{-3} M_J$), suggesting that CO will exist as long as it is sufficiently shielded from stellar UV.

Approximately 50 per cent of the CO lines are double-peaked, which we interpret as arising in a Keplerian disc. Comparing a basic model with the CO profiles, we derive outer radii of 20-300 au for the majority of the discs. In most cases these radii are considerably greater than those

derived from continuum SED modelling. These gas-rich isolated discs are found around stars of ages from 3-17 Myr, and spectral types K through to B9. There is no dependence of size with the spectral type. But there is evidence of a correlation between radius and disc mass, with $M_d \propto R_{out}^{2.8}$. Also the outer radius is dependent on disc age: splitting the stars into two age groups, we find stars < 7 Myr in age have discs 3 times larger than those of age 7-20 Myr. The results indicate that gas-rich discs are available to form planets and cometary material for $\sim 10^7$ yr at radii ~ 200 au, and may last a factor of two longer in the inner ~ 75 au region.

In the four largest CO discs, published scattered light images show comparable dust and gas outer radii, suggesting that the scattering dust and molecular gas are co-located within these discs. In only one case (HD141569) is there evidence of a central gas-free region; many of the others show evidence that gas is found down to radii smaller than 30au.

ACKNOWLEDGMENTS

The James Clerk Maxwell Telescope is operated by the Joint Astronomy Centre on behalf of the United Kingdom Particle Physics and Astronomy Research Council, the Netherlands Organisation for Scientific Research, and the National Research Council of Canada. We wish to thank the various observers, particularly the local staff in Hawaii, for staying at the telescope during mediocre weather, allowing the backup programs to be carried out. Some of the data was extracted from the JCMT archive at the Canadian Astronomy Data Center, which is operated by the Dominion Astrophysical Observatory for the National Research Council of Canada's Herzberg Institute of Astrophysics.

7 REFERENCES

- Aikawa, Y., Herbst, E., 2001, *A&A*, 371, 1107
 Augereau, J. C., Lagrange, A. M., Mouillet, D., M nard, F., 2001, *A&A*, 365, 78
 Augereau, J.C., Dutrey, A., Lagrange, A. M., Forveille, T., 2004, *A&A*(submitted)
 Aumann, H.H., Beichman, C. A., Gillett, F. C., de Jong, T., Houck, J. R., Low, F. J., Neugebauer, G., Walker, R. G., Wesselius, P. R., 1984, *ApJ*, 278, L24
 Backman, D.E., Paresce, F., 1993, in Levy, E.H., & Lunine, J.I., eds, *Protostars and Planets III*, Univ. of Arizona, Tucson, p. 1253
 Beckwith, S.V.W., Sargent, A.I., Chini, R.S., Guesten, R., 1990, *AJ*, 99, 924
 Beckwith, S.V.W., Sargent, A.I., 1993, *ApJ*, 402, 280
 Beskrovnaya, N.G., Pogodin, M.A., Miroshnichenko, A.S., Th , P.S., Savanov, I.S., Shakhovskoy, N.M., Rostopchina, A.N., Kozlova, O.V., Kuratov, K.S., 1999, 343, 163
 Boccaletti, A., Augereau, J.-C., Marchis, F., Hahn, J., 2003, *ApJ*, 585, 494
 Brittain, S.D., Rettig, T.W., Simon, T., Kulesa, C., DiSanti, M.A., Dello Russo, N., 2003, *ApJ*, 588, 535
 Calvet, N., D'Alessio, P., Hartman, L., Wilner D., Wlash, A., Sitko, M., 2002, *ApJ*, 568, 1008
 Coulson, I.M., Walther, D.M., Dent, W.R.F., 1998, *MNRAS*, 296, 934
 Dent, W.R.F., Greaves, J.S., Mannings, V., Coulson, I.M., Walther, D. M., 1995, *MNRAS*, 277, L25
 Dent, W.R.F., Walker, H.J., Holland, W.S., Greaves, J.S., 2000, *MNRAS*, 314, 702
 Dominik, C., Dullemond, C.P., Waters, L.B.F.M., Walch, S., 2003, *A&A*, 398, 607
 Dunkin, S.K, Barlow, M.J., Ryan, S.G., 1997, *MNRAS*, 290, 165
 Dunkin, S.K., Crawford, I.A., 1998, *MNRAS*, 298, 275
 Fekel, F.C., Webb, R.A., White, R.J., Zuckerman, B., 1996, *ApJ*, 462, L95
 Fisher, R.S., Telesco, C.M., Pina, R.K., Knacke, R.F., Wyatt, M.C., 2000, *ApJ*, 532, L141
 Fuente, A., Martin-Pintado, J., Bachiller, R., Neri, R., Palla, F., 1998, *A&A*, 334, 253
 Fuente, A., Martin-Pintado, J., Bachiller, R., Rodriguez-Franco, A., Palla, F., 2002, *A&A*, 387, 977
 Grady, C.A., Woodgate, B., Bruhweiler, F.C., Boggess, A., Plait, P., Lindler, D.J., Clampin, M., Kalas, P., 1999, *ApJ*, 523, L151
 Grady, C. A., Devine, D., Woodgate, B., Kimble, R., Bruhweiler, F. C., Boggess, A., Linsky, J. L., Plait, P., Clampin, M., Kalas, P., 2000, *ApJ*, 544, 895
 Greaves, J.S., Mannings, V., Holland, W.S., 2000, *Icarus*, 143, 155
 Heap, S.R., Lindler, D.J., Lanz, T.M., Cornett, R.H., Hubeny, I., Maran, S. P., Woodgate, B., 2000, *ApJ*, 539, 435
 Herbig, G.H., 1960, *ApJSup*, 4, 337
 Holland, W. S., Greaves, J. S., Zuckerman, B., Webb, R. A., McCarthy, C., Coulson, I. M., Walther, D. M., Dent, W. R. F., Gear, W. K., Robson, I., 1998, *Nature*, 392, 788
 Hollenbach, D.J., Yorke, H.W., Johnstone, D., 2000, in Mannings, V., Boss, A., Russell, S.S., eds, *Protostars and Planets IV*, Univ. of Arizona, Tucson, p. 401
 Hollenbach, D.J., Takahashi, T., Tielens, A.G.G.M., 1991, *ApJ*, 377, 192
 Jayawardhana, R., Fisher, R.S., Telesco, C.M., Pina, R.K., Barrado y Navascu s, D. Hartmann, L.W., Fazio, G.G., 2001, *AJ*122, 2047
 Kalas, P., Graham, J.R., Beckwith, S.V.W., Jewitt, D.C., Lloyd, J., 2002, *ApJ*, 567, 999
 Kamp, I., van Zadelhoff, G.-J., van Dishoeck, E.F., Stark, R., 2003, *A&A*, 397, 1127
 Kastner, J.H., Zuckerman, B., Weintraub, D.A., Forveille, T., 1997, *Science*, 277, 67
 Lisse, C., Schultz, A., Fernandez, Y., Peschke, S., Ressler, M., Gorjian, V., Djorgovski, S.G., Christian, D.J., Golisch, B., Kaminski, C., 2002, *ApJ*, 570, 779
 Li, A., Lunine, J.I., 2003, *ApJ*, 594, L987
 Liseau, R., 1999, *A&A*, 348, 133
 Malfait, K., Bogaert, E., Waelkens, C., 1998, *A&A*, 331, 211
 Mannings, V., Barlow, M.J., 1998, *ApJ*, 497, 330
 Mannings, V., Sargent, A.I., 1997, *ApJ*, 490, 792
 Mannings, V., Koerner, D. W., Sargent, A. I., 1997, *Nature*, 388, 555
 Mannings, V., Sargent, A.I., 2000, *ApJ*, 529, 391
 Matsuyama, I., Johnstone, D., Hartman, L., 2003, *ApJ*, 582, 893

- Meeus, G., Waters, L.B.F.M., Bouwman, J., van den Ancker, M.E., Waelkens, C., Malfait, K., 2001, *A&A*, 365, 476
- Mouillet, D., Lagrange, A.M., Augereau, J.C., Ménard, F., 2001, *A&A*, 372, L61
- Mundy, L.G., Looney, L.W., Welch, W.J., 2000, in Mannings, V., Boss, A., Russell, S.S., *Protostars and Planets IV*, Univ. of Arizona, Tucson, p. 355
- Natta, A., Testi, L., Neri, R., Shepherd, D.S., Wilner, D.J., 2004, *A&A*, 416, 179
- Natta, A., Whitney, B. A., 2000, *A&A*, 364, 633
- Natta, A., Grinin, V. P., Mannings, V., Ungerechts, H., 1997, *ApJ*, 491, 885
- Natta, A., Prusti, T., Neri, R., Thi, W. F., Grinin, V. P., Mannings, V., 1999, *A&A*, 350, 541
- Natta, A., Grinin, V.P., Mannings, V., 2000, in Mannings, V., Boss, A., Russell, S.S., eds, *Protostars and Planets IV*, Univ. of Arizona, Tucson, p. 559
- Natta, A., Prusti, T., Neri, R., Wooden, D., Grinin, V.P., Mannings, V., 2001, *A&A*, 371, 186
- Omodaka, T., Kitamura, Y., Kawazoe, E., 1992, *ApJ*, 396, L87
- Piétu, V., Dutrey, A., Kahane, C., 2003, *A&A*, 398, 565
- Simon, M., Dutrey, A., Guilloteau, S., 2001, *ApJ*, 545, 1034
- Sylvester, R.J., Skinner, C.J., Barlow, M.J., Mannings, V., 1996, *MNRAS*, 279, 915
- Sylvester, R.J., Dunkin, S.K., Barlow, M.J., 2001, *MNRAS*, 327, 133
- Sylvester, R.J., Mannings, V., 2000, *MNRAS*, 313, 73
- Takeuchi, T., Lin, D.N.C., 2001, *ApJ*, 581, 1344
- Testi, L., Natta, A., Shepherd, D.S., Wilner, D.J., 2003, *A&A*, 403, 323
- Thé, P.S., de Winter, D., Perez, M.R., 1994, *A&ASup*, 104, 315
- Thi, W.F., van Dishoeck, E.F., Blake, G.A., van Zadelhoff, G.J., Horn, J., Becklin, E.E., Mannings, V., Sargent, A.I., van den Ancker, M. E., Natta, A., Kessler, J., 2001, *ApJ*, 561, 1074
- Thi, W.F., van Zadelhoff, G.-J., van Dishoeck, E.F., 2004, *A&A*, 425, 955
- Torres, G., 2004, *AJ*, 127, 1187
- van den Ancker, M.E., de Winter, D., Tjin A Djie, H.R.E., 1998, *A&A*, 330, 145
- van Zadelhoff, G.-J., van Dishoeck, E.F., Thi, W.-F., Blake, G.A., 2001, *A&A*, 377, 566
- van Zadelhoff, G.-J., Aikawa, Y., Hogerheijde, M. R., van Dishoeck, E. F., 2003, *A&A*, 397, 789
- Yamashita, T., Handa, T., Omodaka, T., Kitamura, Y., Kawazoe, E., Hayashi, S.S., Kaifu, N., 1993, *ApJ*, 402, L65
- Zuckerman, B., Forveille, T., Kastner, J.H., 1995, *Nature*, 373, 494